



# Actin and Microtubules Play Distinct Roles in Governing the Anisotropic Deformation of Cell Nuclei in Response to Substrate Strain

Dominique Tremblay,<sup>1</sup> Lukasz Andrzejewski,<sup>1</sup> Alexandre Leclerc,<sup>1</sup> and Andrew E. Pelling<sup>1,2,3\*</sup>

<sup>1</sup>Department of Physics, University of Ottawa, Ottawa, Canada

<sup>2</sup>Department of Biology, University of Ottawa, Ottawa, Canada

<sup>3</sup>Institute for Science, Society and Policy, University of Ottawa, Ottawa, Canada

Received 23 May 2013; Revised 7 August 2013; Accepted 26 September 2013  
Monitoring Editor: Pekka Lappalainen

**Physical forces arising in the cellular microenvironment have been hypothesized to play a major role in governing cell function. Moreover, it is thought that gene regulation may be sensitive to nuclear deformations taking place in response to extracellular forces over short and long timescales. Although nuclear responses to mechanical stimuli over long timescales are relatively well studied, the short-term responses are poorly understood. Therefore, to characterize the short-term instantaneous deformation of the nucleus in a mechanically dynamic environment, we exposed MDCK epithelial monolayers to varying mechanical strain fields. The results reveal that nuclei deform anisotropically in response to substrate strain, specifically, the minor nuclear axis is significantly more deformable than the major axis. We show that upon microtubule depolymerization, nuclear deformation anisotropy completely disappears. Moreover, the removal of actin causes a significant increase in nuclear deformation along the minor axis and a corresponding increase in mechanical anisotropy. The results demonstrate that the nucleus deforms in a manner that is very much dependent on the direction of strain and the characteristics of the strain field. Actin and microtubules also appear to play distinct roles in controlling the anisotropic deformation of the nucleus in response to mechanical forces that arise in the cellular microenvironment.** © 2013 Wiley Periodicals, Inc.

**Key Words:** actin; microtubules; strain; nucleus; anisotropy

Additional Supporting Information may be found in the online version of this article.

\*Address correspondence to: Andrew E. Pelling, Department of Physics, University of Ottawa, Ottawa, Canada.

E-mail: a@pellinglab.net

Published online 8 November 2013 in Wiley Online Library (wileyonlinelibrary.com).

## Introduction

It is becoming recognized that the mechanical properties of the cell nucleus likely play an important regulatory role in mechanosensitive gene expression and transcriptional activity [Dahl et al., 2008; Shivashankar, 2011]. Moreover, the nucleoskeleton and proteins of the linker of nucleoskeleton and cytoskeleton (LINC) complexes are phenotypically impaired in developmental defects and diseases such as Hutchinson-Gilford progeria syndrome (HGPS), Emery-Dreifuss muscular dystrophy (EDMD), dilated cardiomyopathy, premature aging and cancer [Sullivan et al., 1999; Lammerding et al., 2004; Chiquet et al., 2009; Coffinier et al., 2011]. It is thought that these genetic defects impair mechanosensory pathways due to altered interactions between transcription factors or increased nuclear fragility [Dahl et al., 2008; Shivashankar, 2011]. In fact, both of these hypotheses are not mutually exclusive and may be interrelated through complex nuclear mechanotransduction mechanisms involving mechanical and biochemical stimuli.

In earlier studies, it was quickly recognized that a physical connection exists between the extracellular matrix and the nucleus. It has been shown that pulling on transmembrane integrins can induce nuclear deformation [Maniotis et al., 1997]. More recent work has shown that the nucleoskeleton is physically linked to the cytoskeleton via LINC complexes [Crisp et al., 2006; Razafsky and Hodzic, 2009]. SUN-1 and SUN-2 are trans-nucleomembrane proteins that make the link between the nucleoskeletal lamins [Haque et al., 2010] and the nesprin proteins, which mainly bind to the cytoskeletal proteins. Nesprin-1 and nesprin-2 interact with actin and microtubules via motor proteins such as dynein [Starr and Fridolfsson, 2010], whereas nesprin-3 binds to intermediate filaments via the adaptor protein plectin [Wilhelmsen et al., 2005].

In-vivo, tissue-embedded cells are exposed to mechanical forces and strains that vary both spatially and temporally.

In-vivo tissue strains are often cyclic and more importantly multi-axial. A good example is the mechanical behaviour of the vasculature walls in response to hemodynamic forces. The focal nature of the hemodynamic forces in the vascular tree [Haga et al., 2007; Frydrychowicz et al., 2008; Barker et al., 2010] combined with the anisotropic properties of vascular tissues [Vande Geest et al., 2006; Tremblay et al., 2009, 2010; Duprey et al., 2010] induce local variations in the mechanical microenvironment exposing endothelial and smooth muscle cells to complex multi-axial and cyclic strain fields. A number of studies have also demonstrated the response of cells to mechanical stretch [Steward et al., 2011; Boccafosci et al., 2011; Balachandran et al., 2011; Rosenzweig et al., 2012]. Importantly, mechanical forces result in rapid, short-term (seconds—minutes) followed by long-term remodeling of the cytoskeleton [Guolla et al., 2012] and nucleus [Booth-Gauthier et al., 2012]. While the longer term effects of mechanical stimulation have been intensively studied, the short-term effects are relatively poorly understood.

Numerous stretching experiments have greatly contributed to the basic understanding of mechanotransduction and mechanobiology, but they have traditionally relied on idealized uniaxial or equi-biaxial strain fields that may not reproduce complex in-vivo strain fields [Yang et al., 2004; Haga et al., 2007; Jungbauer et al., 2008; Goldyn et al., 2009; Steward et al., 2011; Boccafosci et al., 2011; Balachandran et al., 2011; Heo et al., 2011; Rosenzweig et al., 2012]. In addition, standard uniaxial stretching experiments also induce a compressive strain perpendicular to the stretching direction. This additional compressive strain is often ignored, making it difficult to interpret the effect of the substrate strain on nuclear deformability.

Interestingly, recent work has indicated that the nucleus possesses an anisotropic mechanical prestress caused by an increased number of nucleo-cytoplasmic contacts at the ends of nuclei [Mazumder and Shiva-shankar, 2010]. Laser ablation of heterochromatin nodes caused elliptical nuclei to shrink significantly more along their minor axis compared to their major axis. Given that nuclei appear to be anisotropically prestressed we hypothesized that they should deform anisotropically along the major and minor axes in response to substrate stretch. It was also observed that prestress and anisotropy increases during differentiation. Clearly, the mechanical properties of the nucleus are not only linked to mechanosensory pathways in health and disease but also appear to be highly anisotropic. Importantly, studies of nuclear deformability in response to substrate strains have not specifically examined how the nucleus deforms along each axis. Therefore, it remains unclear if forces that arise in-vivo also cause anisotropic deformation of cell nuclei. Given that the nucleus may act as a mechanosensor it is important to understand how the nucleus deforms in response to extra-cellular forces.

To systematically examine how the nucleus deforms in response to substrate stretch, we built a biaxial stretching (BAXS) device that allows for simultaneous live-cell microscopy. Employing this device, our objectives were to examine how cell nuclei deform along their major and minor axes, characterize how nuclear deformation varies in compressive and non-compressive strain fields and to investigate the role of the actin and microtubule cytoskeleton in regulating nuclear deformation. Importantly, as cyclical stretching is known to cause significant remodelling effects in the nucleus and cytoskeleton, we examined the instantaneous deformation of the nucleus in response to a constant 25% substrate stretch. This allowed us to characterize how an unperturbed cytoskeleton modulates the deformation of the nucleus prior to the onset of any dramatic remodeling effects. We demonstrate that MDCK nuclei are significantly more deformable along the minor axis compared to the major axis. This deformation anisotropy is also enhanced in a non-compressive strain field. In addition, it was observed that actin tends to resist deformation along the minor axis whereas microtubules tend to resist deformation along the major axis. The results show that the nucleus deforms in a manner that is dependent on the direction of strain and the state of the cytoskeleton. Distinct cytoskeletal elements appear to play an important role in modulating how much the nucleus deforms in response to mechanical forces that arise in the microenvironment.

## Results

### Generating Compressive and Non-Compressive Uniaxial Strain Fields

In order to expose cells to compressive and non-compressive uniaxial strains, we cultured them on a PDMS membrane that could be stretched along two orthogonal directions (Materials and Methods). The membrane was mounted on a custom-built BAXS device shown in Fig. 1A that allowed us to monitor cell and organelle deformations during exposure to constant planar stretching (Figs. 1B–1G). A compressive uniaxial strain field is induced by stretching along the horizontal axis only, which in turn causes compression along the vertical (orthogonal) axis (Fig. 2A). Compressive uniaxial strain fields have been commonly employed in many previous studies when examining cellular response to substrate strain [Boccafosci et al., 2011; Balachandran et al., 2011]. Conversely, to induce a non-compressive uniaxial strain field, the membrane is stretched along the axis orthogonal to the principal stretching axis (Fig. 2B). This compensatory orthogonal stretch causes the compression strain to approach zero.

In brief, phase contrast images of the cells and fluorescence images of nuclei were acquired before stretching and retained as a reference shape (Figs. 3A and 3D). At first, cells were exposed to a constant 25% compressive uniaxial strain along

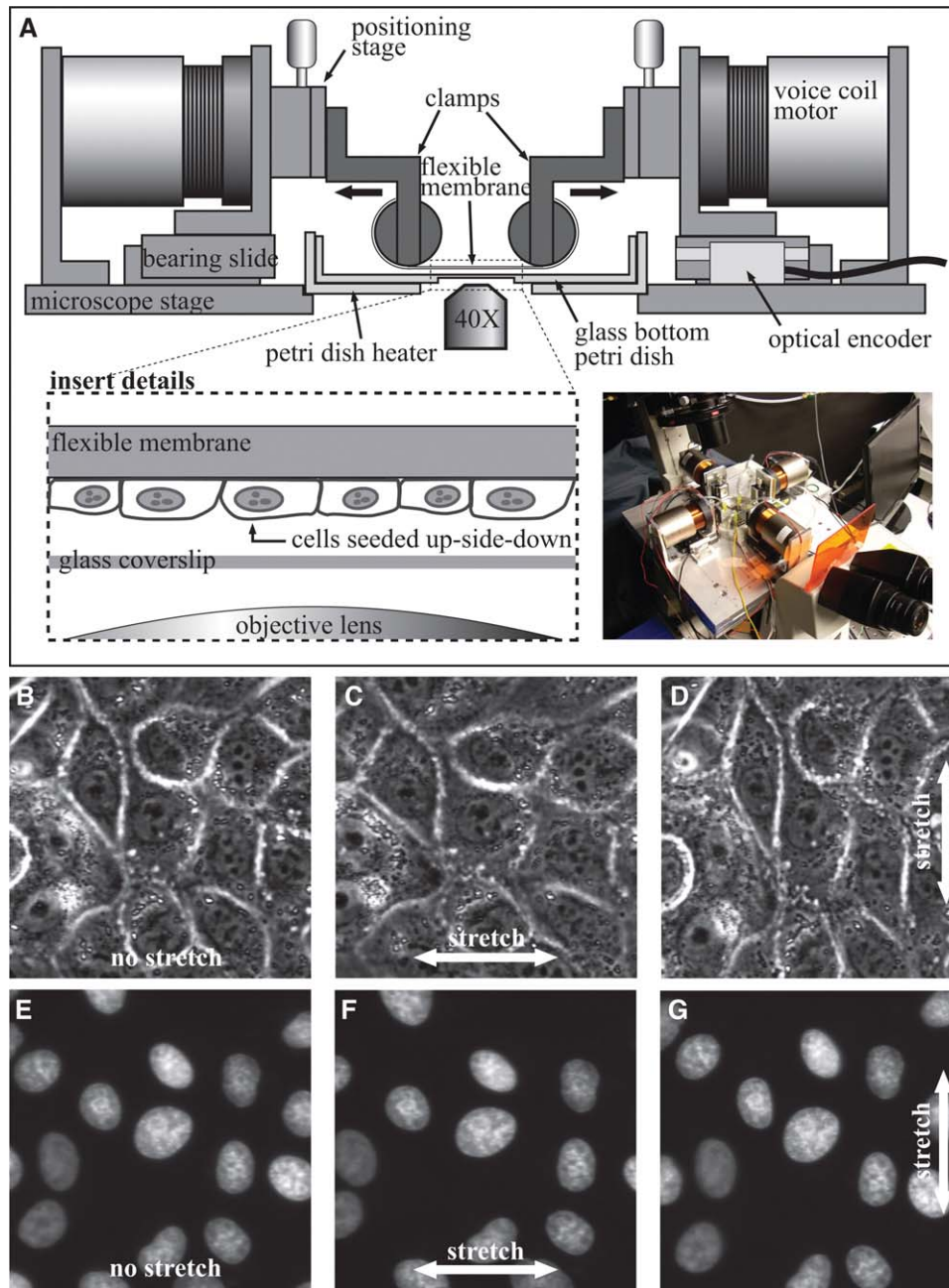


**Fig. 1. Details of the cell stretching device and its working principles.** (A) Side view drawing of the custom-built anisotropic BAXS showing the motorized stages with the clamping system that holds the flexible silicon membrane in place and on which cells are seeded. (see insert) This membrane is carefully positioned at about 300  $\mu\text{m}$  from the surface of a glass bottom petri dish to bring the cells as close as possible to the microscope objective. (B–D) Phase contrast images of the same cells showing substrate strain in the horizontal and vertical direction. (E–G) Epi-fluorescent images of cell nuclei labelled with a DNA-specific dye. This image sequence illustrates a typical cell stretching experiment where the same group of cells is exposed to two strain fields.

the horizontal axis followed by a constant 25% compressive uniaxial strain along the vertical axis (Figs. 3B and 3C). The same group of cells was then exposed to a constant 25% non-compressive uniaxial strain along the horizontal axis followed by a constant 25% non-compressive uniaxial strain along the vertical axis (Figs. 3E and 3F). It is important to note that cells were exposed to a constant strain, as opposed to a cyclical strain. Over long periods of time, cyclical stretching is well known to result in large scale remodelling of the

cytoarchitecture [Goldyn et al., 2009; Ngu et al., 2010; Morioka et al., 2011]. In this study our objective was to understand the role of the cytoskeleton in modulating the instantaneous deformation of the nucleus.

### Actin and Microtubules Resist Nuclear Deformation in Response to Substrate Strain

To examine the role of the cytoskeleton in regulating nuclear deformation in response to substrate strain we

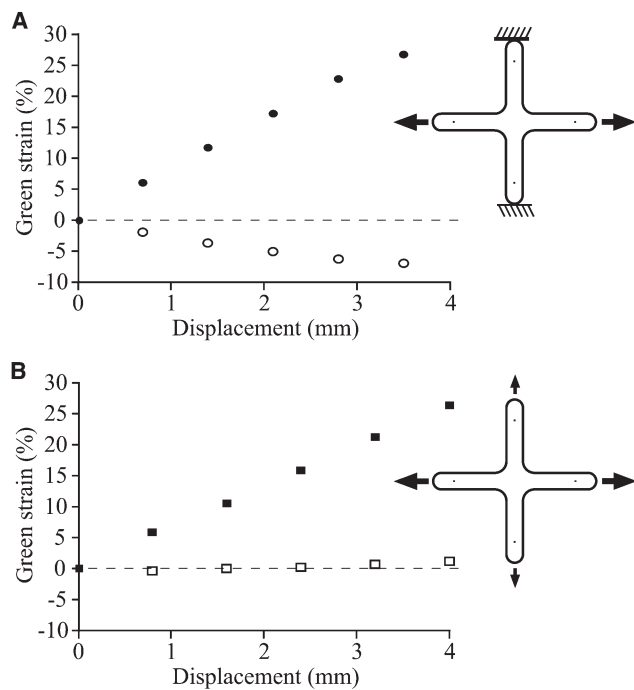


**Fig. 2. An example of two calibration curves for two different strain fields.** (A) Calibration curve for a compressive uniaxial strain field where the membrane is stretched along the horizontal axis by 3.5 mm on each end while keeping the ends along the vertical axis fixed. The filled circles illustrate the linear and positive relationship between the horizontal component of the Green strain tensor in respect to the motor displacement along the horizontal direction. The empty circles illustrate the vertical component of the Green strain tensor showing a linear and compressive strain in respect to the motors displacement along the horizontal axis. (B) Calibration curve for a non-compressive uniaxial strain field where the membrane is stretched along the horizontal axis by 4 mm and by 1.5 mm along the vertical axis. The filled squares illustrate the linear and positive relationship between the horizontal component of the Green strain tensor in respect to the motor displacement. The empty squares illustrate the vertical component of the Green strain tensor showing a zero strain value with motors displacement.

employed cytochalasin-D and nocodazole to specifically depolymerize the actin network and the microtubules, respectively (see Fig. S1 in Supporting Information). We note that actin stress fibers were observed only at the basal level of the cell, whereas the microtubules were present throughout the cell body completely surrounding the nucleus. We found that cytochalasin-D and nocodazole did not affect the structure of the third major component of the cytoskeleton, the intermediate filaments (see Figs. S2B and S2C in Supporting Information). Similar to the microtubules, intermediate filaments were also observed to be present throughout the cell body, completely surrounding the nucleus.

We first examined cell nuclei when exposed to a compressive uniaxial strain field (Figs. 4A and 4B). In these experiments, nuclei were examined and stretched along their major or minor axes. We found that nocodazole had a

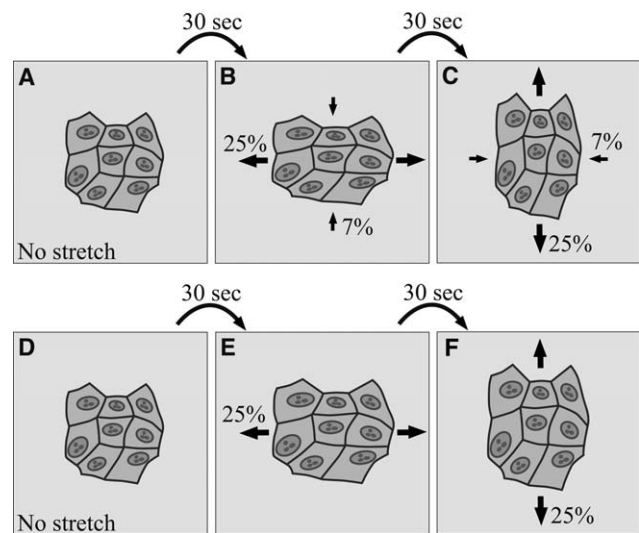


**Fig. 3. This cartoon illustrates a typical cell stretching experiment where the same population of cells is exposed to two types of strain fields.** (A) The group of cells of interest is not exposed to any substrate strain; the nuclear shape of each cell will be used as a reference to compute nuclear deformation during substrate strain. (B) The same population of cells is then exposed to a 25% compressive uniaxial strain field oriented horizontally with a natural vertical substrate compression of 7%. (C) Then the cells are further exposed to the same strain field than in (B) but rotated by 90°. Following this, the same group of cells is exposed to the second type of strain field: a non-compressive uniaxial strain field. (D) no substrate strain; the nuclear shape of each cell will be used as a reference to compute nuclear deformation during substrate strain. (E) The same cells are exposed to a 25% non-compressive uniaxial strain field oriented horizontally but with no substrate compression along the vertical direction. (F) Then cells are exposed to the same strain field than in (E) but rotated by 90°.

significant effect on the nuclear deformability when stretched along the major axis, but not along the minor axis, compared to nuclei in untreated cells ( $5.8 \pm 0.7\%$  and  $3.6 \pm 0.5\%$ , respectively; Fig. 4A). On the other hand, cells treated with cytochalasin-D exhibit a significantly higher nuclear deformability when stretched along the minor axis, but not along the major axis, in comparison to control cells ( $7.1 \pm 0.6\%$  and  $5.2 \pm 0.6\%$ , respectively; Fig. 4B). These results indicate that the microtubule and actin network both contribute to minimizing nuclear deformation when cells are exposed to substrate strain but do appear to have two distinct roles. Actin appears to resist minor axis deformation and microtubules appear to resist major axis deformation.

The BAXS device then allowed us to expose the same group of cells to a non-compressive uniaxial strain field. As above, when stretched along the major axis, treatment with nocodazole resulted in a significantly higher nuclear deformation as compared to untreated cells ( $7.1 \pm 0.7\%$  and  $4.4 \pm 0.6\%$ , respectively; Fig. 4C). However, cells treated with cytochalasin-D or nocodazole revealed no significant change in deformability compared to untreated cells (Fig.

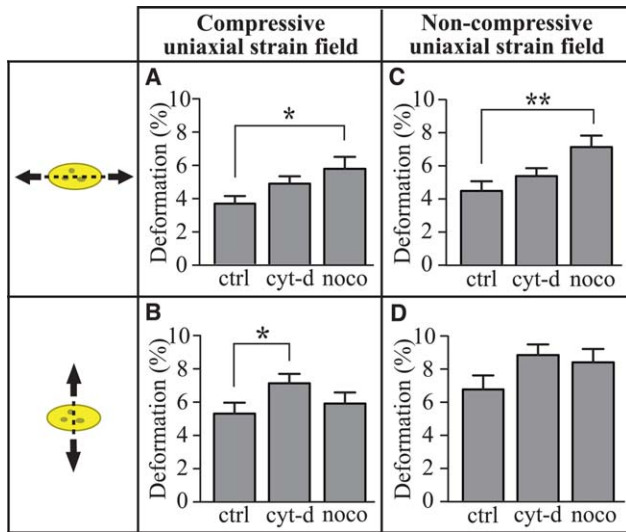


**Fig. 4. Nuclear deformation of cells stretched along the major axis and minor axis of their nucleus.** The cartoon on the right indicates the stretching direction (black arrows) and which axis of the nucleus is being measured (dotted line). Nuclear deformation along the major during nocodazole treatment is significantly greater than in control cells for both types of strain fields: (A) compressive and (C) non-compressive uniaxial strain field. Whereas cytochalasin-D induces a significant increase in nuclear deformability along the minor axis during a compressive uniaxial stretching experiment only (B). \*  $P$ -value  $< 0.05$ , \*\*  $P$ -value  $< 0.01$ , one-way ANOVA followed by Tukey post-test. [Color figure can be viewed in the online issue which is available at [wileyonlinelibrary.com](http://wileyonlinelibrary.com).]

4D). When comparing the nuclear deformation between cells exposed to a compressive and non-compressive strain field, we observed a general increase in the magnitude of the deformation. Indeed, this increase is significant for the major and minor axis and for both cytoskeletal drugs (see Fig. S3 in Supporting Information). Therefore, the absence of compression in a uniaxial strain field results in a larger nuclear deformation.

### Nuclei Deform Anisotropically

In addition to the results above, the data also demonstrates that the minor axis always deforms significantly more than the major axis in either a compressive or non-compressive strain field. This behaviour indicates that the nucleocytoskeleton system possesses anisotropic mechanical properties that lead to anisotropic deformation of the nucleus. Cells exposed to an equi-biaxial strain field (25% substrate strain along both the vertical and horizontal axes) confirmed that the anisotropic deformation of the nuclei persists and is not only a result of compressive or non-compressive strain fields (see Supporting Information). Here, we define an anisotropic index (AI) to quantify the variation in nuclear deformability between the major and minor axes. This index is simply computed as the difference between the deformability of the minor and the major axis of the nucleus ( $AI = \text{minor axis deformation} - \text{major axis}$

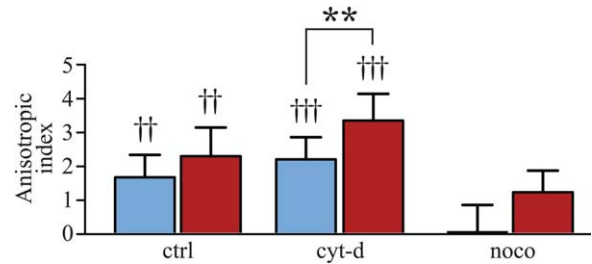


**Fig. 5. The anisotropic index is computed as the difference between the deformability of the minor and major axes.** A positive index means that the minor axis deforms more than the major axis. Control and cytochalasin-D-treated cells show anisotropic deformability since their AI are significantly different from zero for both types of strain field (dagger symbol). Blue and red bars correspond to compressive and non-compressive strain fields. However, cells treated with nocodazole show isotropic deformability. \*\*  $P$ -value  $< 0.01$ , paired  $t$ -test. ††  $P$ -value  $< 0.01$ , †††  $P$ -value  $< 0.001$ , one-sample  $t$ -test. [Color figure can be viewed in the online issue which is available at [wileyonlinelibrary.com](http://wileyonlinelibrary.com).]

deformation). Therefore, a positive AI indicates a higher deformability of the minor axis than the major axis (Fig. 5). On average, the AI was positive for all conditions, but only control and cytochalasin-D treated cells differed significantly from zero under compressive and non-compressive uniaxial strain fields. This indicates that exposure to nocodazole (loss of microtubules) results in a loss of anisotropic deformation. Moreover, in response to cytochalasin-D (loss of actin) we observed a significant increase in AI in a non-compressive strain field compared to a compressive strain field. These results indicate that the presence microtubules are required to maintain anisotropic nuclear deformability. When microtubules are disrupted, nuclei deform isotropically due to the increase in deformability along the major axis while the minor axis deformability remains the same.

### Microtubules Resist Compressive Loading in Compressive Uniaxial Strain Field

In the above sections, we examined the deformability of the major and minor nuclear axes when oriented parallel to the principal stretching axis. We now consider the deformation of the major and minor nuclear axes when oriented perpendicular to the principal stretching axis. In other words, when cells were stretched along the major axis of the nucleus, we quantified the deformation of the minor nuclear axis (Fig. 6). By investigating nuclear deformation perpendicular to the principal stretching axis, we can quantify the effect of the compressive strain that arises in a uniaxial strain field (Fig. 6). A negative response indicates that the nuclei are compressed along their major and minor axes respectively (Figs. 6A and 6B). Indeed, when stretching cells along the minor axis of their nucleus, the major axis of control cells shrinks by  $-1.4 \pm 0.3\%$  (Fig. 6A). Similar behaviours were observed in cytochalasin-D- and nocodazole-threaded cells ( $-1.4 \pm 0.4\%$  and  $-1.9 \pm 0.5\%$ ,

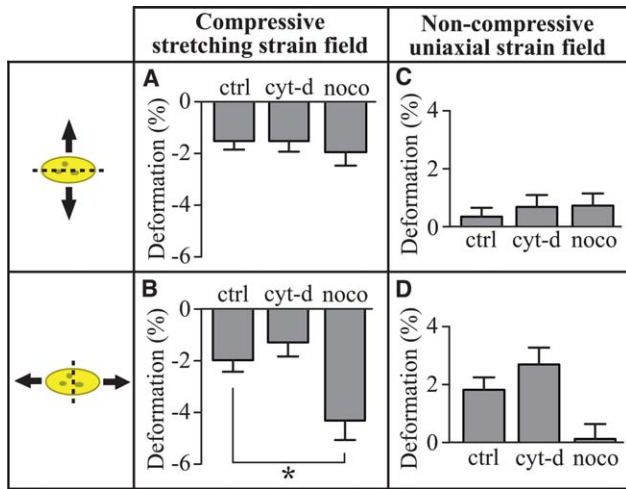


**Fig. 6. Nuclear deformation of cells stretched across the major axis and minor axis of their nucleus.** The cartoon on the right indicates the stretching direction (black arrows) and which axis of the nucleus is being measured (dotted line). (A) The negative values indicate the shrinkage of the major axis during stretching along the minor axis of the nucleus and (B) the shrinkage of the minor axis during stretching along the major axis of the nucleus. Nocodazole treatment induces a significant shrinkage of the minor axis but has no effect on the major axis during compressive uniaxial stretching experiment. The removal of the compressive strain field during non-compressive uniaxial stretching experiments results in the stretching of the nucleus (C and D). \*  $P$ -value  $< 0.05$ , \*\*  $P$ -value  $< 0.01$ , one-way ANOVA followed by Tukey post-test. [Color figure can be viewed in the online issue which is available at [wileyonlinelibrary.com](http://wileyonlinelibrary.com).]

respectively). On the other hand, when cells were stretched along the major axis we found that the minor axis in nocodazole-treated cells decreased significantly more than control cells ( $-4.3 \pm 0.7\%$  and  $-1.9 \pm 0.4\%$ , respectively; Fig. 6B). Interestingly, the absence of microtubules significantly increases the deformability of the minor axis when the cells were stretched parallel to the major axis. These results indicate that microtubules appear to resist the compressive loading arising from the substrate during compressive uniaxial stretching.

Additional experiments were then performed in which cell monolayers were exposed to a non-compressive uniaxial strain field (Figs. 6C and 6D). Indeed, a non-compressive strain field did not cause the nucleus to shrink along the axis perpendicular to the principal stretch direction. When nuclei were stretched along the minor axis, the major axis only exhibited about 0.6% deformation for control and drug treated cells with no significance between them (Fig. 6C). When nuclei were stretched along the major axis, the minor axis increased slightly in control and cytochalasin-D-treated cells ( $1.8 \pm 0.4\%$  and  $2.6 \pm 0.6\%$  respectively). Nocodazole treated cells exhibited no significant change in deformation compared to the undeformed state (Fig. 6D).

## Discussion

In this study we investigated the effect of substrate strain and the specific role of actin and microtubules in modulating the deformation of nuclei in MDCK monolayers. In recent work, it has been demonstrated that extracellular forces (shear stress and compression) result in the dynamic reorganization of the chromatin over two distinct timescales [Booth-Gauthier et al., 2012]. In the short-term ( $< 30$  min) intranuclear movements of the DNA are suggested to be driven by a combination of mechanical stress, cytoskeletal reorganization and signaling dynamics. However, in the long-term ( $> 30$  min) reorganization of the genome and altered gene expression dynamics are affected. In contrast to the short-term results presented in this study, we also performed an additional experiment in which cells were exposed to a constant 25% stretch for a 20-min time period. During longer exposure to substrate stretch, nuclear remodelling was clearly observed (see Fig. S4 in Supporting Information). The nucleus deforms anisotropically under the initial substrate deformation and then slowly remodels and shrinks toward its original shape while keeping its anisotropic shape consistent with the timescales of previous work [Booth-Gauthier et al., 2012]. Clearly, nuclear structure can remodel and adapt accordingly to its new mechanical microenvironment over longer time scales. However, the present study was designed to investigate short-term effects of substrate stretch in order to characterize how cytoskeletal proteins contribute to anisotropic nuclear deformation.

In general, it has been assumed that nuclei are fairly isotropic structures but recent evidence works has suggested that their mechanical properties are anisotropic [Mazumder and Shivashankar, 2010]. In committed cells, nuclei are generally elliptical, possessing a clear geometric anisotropy. Employing laser ablation, destruction of heterochromatin nodes resulted in an anisotropic shrinkage of the nucleus. The actin and microtubule cytoskeleton and activity of myosin-II were observed to be major contributors to the mechanical anisotropy of the nuclei. Moreover, nuclear prestress, which drives anisotropy, was observed to increase during differentiation and development. Therefore, given that nuclear mechanotransduction and mechanosensitivity play such important roles in-vivo, it is critical to understand the anisotropic behaviour of the nucleus, especially in response to extracellular deformation.

Upon microtubule depolymerization, anisotropic deformation of the nucleus completely disappeared in both compressive and non-compressive strain fields. The loss of anisotropy is due to a significant increase in major axis deformation in both scenarios. The deformation of the nuclear minor axis does not change significantly compared to untreated cells in both compressive and non-compressive uniaxial strain fields. In addition, when monitoring the nuclear response perpendicular to the stretching direction, microtubule-deprived cells displayed an increased

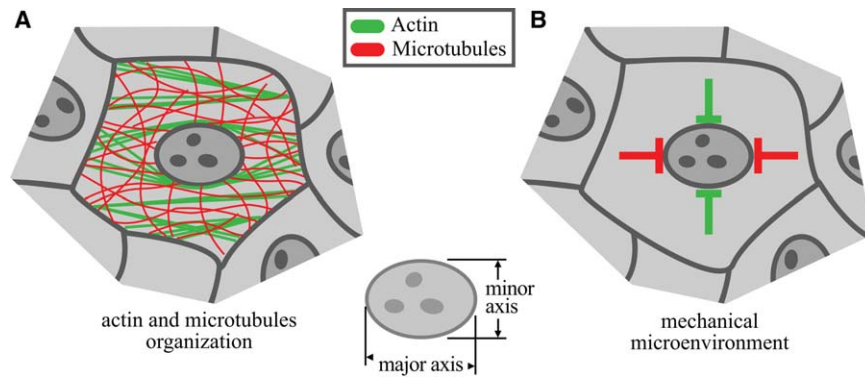


**Fig. 7. An illustration of the contributions of actin and microtubules to modulating anisotropic nuclear deformation during substrate stretching.** (A) Polarized actin fibers surrounding the nucleus only at the basal level whereas microtubules are found throughout the cell at the basal and apical levels. (B) These contributions of the actin and microtubule cytoskeleton to the anisotropic deformation of the nucleus are shown here schematically. It was observed that when actin is depolymerized, the nucleus deforms significantly more along the minor axis but when microtubules are depolymerized the nucleus deforms significantly more along the major axis. Actin and microtubules appear to prevent nuclear deformation along the minor and major axes respectively. The microtubules appear to offer a greater resistance to deformation than the actin fibers, which results in a nucleus that is more deformable along its minor axis than its major axis.

deformability along the nuclear minor axis. Significant compression of the minor axis is the result of increased elongation of nuclei along the major axis due to its higher deformability but also from the likely ability to expand perpendicular to the substrate plane in the absence of microtubules above the nucleus. As such, it appears that microtubules play an important role in controlling anisotropic nuclear deformation (Fig. 7). Conversely, in a compressive uniaxial strain field the loss of actin led to increased nuclear deformation when stretched along the minor axis compared to untreated cells. Conversely, the loss of actin had no significant effect on nuclear deformation when stretched along the major axis. In a non-compressive strain field, the loss of actin had no statistically significant effect on nuclear deformation (compared to untreated cells) when stretched along either axis. However, minor axis deformation increased significantly compared to cells in a compressive uniaxial strain field. Therefore, actin appears to play a role in preventing nuclear deformation along the minor axis (Fig. 7).

It has been shown that depolymerization of actin can result in a reduction of nuclear deformation in endothelial cell monolayers when exposed to compressive uniaxial strain field [Nathan et al., 2011; Anno et al., 2012]. In this previous work, cells were cultured on patterned substrates in order to preferentially align them with the stretching direction. It has been shown that confining cell orientation results in the remodelling of the cytoskeleton in concert with nuclear shape [Versaevol et al., 2012]. Therefore, we expect that the mechanical response of aligned endothelial nuclei to be different from a randomly aligned monolayer of epithelial cells.

In compressive and non-compressive uniaxial strain fields, nuclei of untreated cells also clearly exhibited a significant deformation anisotropy. Interestingly, although

nuclei deformed anisotropically, the entire cell deformed isotropically (see Fig. S5 in Supporting Information). It should be noted that although substrate strain does have a major impact on the organization of the cytoarchitecture, only a fraction of the substrate strain is transferred to the nucleus. On average, only 15–30% of the substrate strain was converted into nuclear deformation, which is in agreement with previous work [Arnoczky et al., 2002; Anno et al., 2012]. Such mechanical behaviour suggests that the mechanical links between the nucleus and the substrate are more deformable than the nucleus itself. Although the actin fibers and microtubules are load-bearing structures capable of force transmission from the extracellular matrix to the nuclear envelope, our results suggest that forces they transmit to the nucleus is limited because of their significantly smaller cross-sectional area in comparison to the nucleus. This results in the incapacity of the cytoskeleton to transmit all the stress to the nucleus, which is translated into the deformation of the cytoskeleton. This suggests that a relatively large microenvironmental strain is required to induce a deformation of the cellular genome. As suggested previously, it is likely that there is a combination of events in which mechanical signals are transduced into changes in gene expression [Reddy et al., 2008; Szczerbal et al., 2009; Korfali et al., 2010]. These events may occur through direct deformation of the cell nucleus and/or through short-term deformation of the cytoskeleton and downstream biochemical signaling [Guolla et al., 2012; Booth-Gauthier et al., 2012].

Anisotropic nuclear deformation was also found during equi-biaxial stretching which indicates that the anisotropy we observed was not the result of exposing a cell to uniaxial strain fields (see Fig. S6 in Supporting Information). We also monitor the displacement of the internal structures of the DAPI-stained nucleus using the distinct features

corresponding to high or low DNA content regions. The internal structures were found to deform anisotropically following the overall change in shape for the nucleus. In general, nuclei were found to deform 50% more along the minor axis than the major axis. Importantly, the AI was not observed to differ significantly in a compressive or non-compressive strain field. Additionally, depolymerizing actin or microtubules causes an isotropic shrinking of the nucleus (see Fig. S7 in Supporting Information) and in the absence of substrate stretch, the anisotropic properties of the nucleus are not apparent. Only after exposure to substrate stretch does it become clear how actin and microtubules modulate the deformation of the nucleus. The following qualitative picture emerges when considering the observations of this study (Fig. 7): When stretched along the major axis, microtubules appear to resist deformation (expansion). On the other hand, when stretched along the minor axis, actin fibers appear to prevent nuclear deformation. The anisotropic deformation of the nucleus may be explained by the greater capacity of the microtubules to resist nuclear deformation than actin. This may be due to the fact that microtubules completely surround the nucleus and the actin is only found at the basal level. Also, actin is generally polarized parallel along the major axis, acting to prestress the nucleus having a major influence in preventing expansion of the minor axis.

Clearly, actin and microtubules appear to play differential roles in regulating the anisotropic deformation of the nucleus. It has been shown that when actin is depolymerized, the nucleus acquires a spherical shape indicating that the nucleus is mechanically prestressed [Mazumder and Shivashankar, 2010]. In single adherent cells (fibroblasts) such prestress is thought to cause the nucleus to be pulled tightly towards the basal membrane of the cell via actin stress fibers that cap the nucleus on the apical side. Indeed, it has been recently demonstrated that the actin cap plays a major role in governing nuclear shape [Khatau et al., 2009, 2012; Kim et al., 2012]. In MDCK monolayers, we found no clear actin cap present but the presence of a microtubule and intermediate filament cap. This may explain why the removal of actin induces an increase in nuclear deformation as opposed to a reduction [Anno et al., 2012]. Unlike single cells, the morphology and structure of epithelial monolayers may not require the same amount of tension present in single contractile cells [Khatau et al., 2009]. As a consequence, we hypothesize that the loss of actin may weaken the interactions between the nucleus, microtubules and intermediate filaments causing the minor axis to become more deformable [Versaevl et al., 2012]. However, in previous work, the tension of actin, which runs over the nucleus, has been implicated in the origin of the normal force [Anno et al., 2012]. As mentioned earlier, no apical actin stress fibers are present in the MDCK monolayer but microtubules and intermediate filaments are clearly present above the nucleus. It is

unclear which component of the cytoskeleton induces this normal stress on the nucleus as the depolymerization of the microtubules or actin did not significantly reduce the minor and major elongation during stretch. However, the intermediate filaments are a likely candidate as they play a major role in governing the mechanical properties of epithelial cells [Herrmann et al., 2007]. Increased tension in the intermediate filament network may induce a normal compressive force on the nucleus, causing larger deformations along the major and minor axes in the substrate plane.

Taken together, our study has several important implications on our understanding of the influence of physical and mechanical stimuli on cell function. The nucleus of epithelial cells deforms anisotropically which may have an important role in governing changes in gene expression due to a mechanical stimulus. This deformation takes place over relatively short timescales (seconds) and thus may play an important role in the ultimate downstream genomic response (hours to days) [Booth-Gauthier et al., 2012]. Moreover, actin and microtubules appear to play differential roles in regulating the deformation of the nucleus. The loss of actin clearly increases the anisotropic deformation of the nucleus and the loss of tubulin completely inhibits anisotropic deformation. Epithelial cells appear to be highly sensitive to subtle changes in the characteristics of the strain field (compressive and non-compressive) resulting in significant changes in nuclear deformation. These results, and the work of others described above, leads us to speculate that these cells may regulate their sensitivity to microenvironmental strain by altering actin and microtubule organization and in turn, anisotropic deformation of the nucleus.

## Materials and Methods

### Anisotropic Biaxial Stretching Device

To perform the present study, a custom biaxial stretcher (BAXS) was constructed and integrated onto an inverted phase contrast and fluorescence microscope (Nikon Ti-E, Nikon Canada). The BAXS was designed to allow the stretching of a flexible membrane along two perpendicular axes in order to produce fully controllable isotropic and anisotropic biaxial strain fields. The design also allowed for simultaneous imaging of cellular deformation during strain application. In order to implement this design, a flexible membrane was fabricated using a cross-shaped SU-8 mould made from photolithography techniques. A flexible membrane was produced from polydimethylsiloxane (PDMS, Sylgard 184 Kit, Dow Corning), which was embedded with 200 nm fluorescent beads that later enabled real-time tracking of the strain field during an experiment. Red fluorescent beads (FluoSpheres, 200 nm, Invitrogen, CA) in a water suspension were resuspended in isopropanol at a ratio of

10:1. A 30- $\mu$ l drop of the bead solution was added to the PDMS cross-linker solution and vortexed. The PDMS was mixed at a ratio of 20:1 with cross-linking solution and poured by weight into the SU-8 mould. The PDMS was cured at 80 °C for 2 h, producing a uniform 300  $\mu$ m thick cross-shaped membrane that could then be functionalized to promote cell adhesion. The BAXS consisted of four linear voice coil motors (Moticont, CA) each mounted on a miniature linear motion ball bearing slide (Edmund Optics, NJ) and oriented along two perpendicular axes (Fig. 1A). A linear positioning stage (Edmund Optics) was mounted to each of the four motors. In turn, each of the four arms of the cross-shaped membrane were clamped and mounted to a single linear positioning stage. This assembly allowed us to minimize the distance between the microscope objective and the cells to enable high-resolution imaging (see insert in Fig. 1A). The position of each motor was recorded by an optical encoder with a resolution of 500 nm (MicroE Systems, MA). All four motors were independently controlled with a motion controller (DMC-2143, Galil, CA) employing optical encoder feedback to execute motion commands. A LabView interface allowed the user control over the displacement magnitude, speed and acceleration of each motor in order to generate completely customizable, static and dynamic, isotropic and anisotropic biaxial strain fields.

### Generating Compressive and Non-Compressive Uniaxial Strain Fields

Prior to each stretching experiment, calibration-stretching cycles were performed to characterize the relationship between the displacements of the voice coil motors and the measured strain field in the flexible membrane (Fig. 2). A MATLAB script allowed us to compute the Green strain tensor in the plane of the PDMS membrane by tracking the position of the embedded fluorescent beads during stretching (see Supporting Information and Fig. S8 in Supporting Information). Typically, a 4 mm displacement produced, on average, a 25% strain along the horizontal or vertical axis. Exploiting the ability to independently control the displacement along each orthogonal axis allowed us to either expose cells to compressive or non-compressive uniaxial strain fields. A non-compressive uniaxial strain field was through a 4 mm displacement along the principal stretching axis combined with a 1.5 mm displacement along the orthogonal axis. Over the course of single stretching experiments, we observed a standard deviation of at most  $\pm 0.1\%$  on the strain magnitude. This indicates that the membrane was properly fixed to the four clamps mounted on the voice coils and displayed no slip behaviour. Moreover, this also confirms that all cells tested were exposed to the desired strain field during the multiple stretching cycles. However, while the cross-shaped geometry of the flexible membrane allowed us to precisely control the strain along the two orthogonal axes, this does

lead to a non-uniform strain magnitude over the membrane surface. By carefully characterizing the spatial variation of the strain magnitude occurring on the membrane, we found that the central region of the membrane (3 mm in diameter) centered above the microscope objective was relatively constant ( $\pm 0.53\%$  variation in strain magnitude). Therefore, only cells within this region were analyzed during exposure to compressive and non-compressive uniaxial strain fields.

In all experiments, cells were exposed to a constant 25% uniaxial strain along the horizontal axis followed by a constant 25% uniaxial strain along the vertical axis (Fig. 3). The strain rate at which cells were stretched was 1%/s and then the deformation was held constant for 5 s; the time necessary to acquire phase contrast and fluorescence images. Initially, a fluorescent image of the nuclei was acquired under no substrate strain, which was retained as the reference shape (Fig. 3A). Cells were then exposed to a compressive uniaxial strain field along the horizontal axis and a fluorescent image of the deformed nuclei was acquired (Fig. 3B). At this point the membrane was relaxed back to its undeformed state. The same group of cells was then exposed to a compressive uniaxial strain field along the vertical axis and nuclear shape was imaged again (Fig. 3C). Subsequently, the same cell population was then exposed to a non-compressive uniaxial strain field in the same sequence as above. In this case, a compensatory stretch was applied along the axis orthogonal to the principal stretch axis (Figs. 3D–3F). Upon completion of the image acquisition, raw image data were analyzed to quantify the deformation and orientation of the nuclei. We also confirmed that cells stretched multiple times over a 2 min period did not exhibit effects, such as irreversible changes in nuclear morphology (see Supporting Information). We performed paired *t*-tests comparing nuclear shape descriptors (major/minor axis lengths) between stretching cycles to determine if multiple cycles had an irreversible effect on nuclear deformability. Our analysis revealed that no significant differences were found between stretching cycles indicating that under the conditions of this study, nuclear deformation was reversible (see Fig. S9 in Supporting Information). Nuclear shape and size was always observed to return to their initial state indicating that no irreversible remodelling processes were taking place over the timescale of the experiment (see Fig. S10 in Supporting Information).

As shown in Figs. 1B–1G, one can appreciate the whole cell and nuclear deformation that occurs in response to strain. In order to properly investigate the effect of substrate strain on nuclear deformation we only examined nuclei that were oriented within 15° of the horizontal or vertical stretching axis. This approach allowed us to quantify the deformation of the major and minor axes of cell nuclei when aligned parallel or perpendicular to the uniaxial strain direction in a compressive versus a non-compressive strain field.

## Cell Seeding and Nuclei Staining

The PDMS membrane was air plasma treated at 30 W for 30 s to generate hydroxyl groups and enhance collagen binding. The membrane was coated with 5  $\mu\text{g}/\text{cm}^2$  of rat-tail collagen I (Gibco, NY) and incubated at room temperature for 1 h. After rinsing with PBS, MDCK cells were seeded over a 1-cm<sup>2</sup> area on the central portion of the membrane at a final surface density of 500 cells/mm<sup>2</sup> (see Supporting Information and Fig. S11 in Supporting Information). Cells were cultured and suspended in Dulbecco's Modified Eagle Medium (Invitrogen) supplemented with 10% fetal bovine serum (Invitrogen) and 1% penicillin-streptomycin (Invitrogen). Cells were allowed to grow in a monolayer in a standard cell incubator for 48 h (5% CO<sub>2</sub> and 37 °C). Twenty minutes before an experiment, cell nuclei were labelled with a DNA-specific live-cell fluorescent dye, Hoechst 33342 (Invitrogen) according to manufacturer protocols. After 20 min of incubation, cells were washed with a HEPES-buffered salt solution (HBSS; 20 mM of Hepes at pH 7.4, 120 mM of NaCl, 5.3 mM of KCl, 0.8 mM of MgSO<sub>4</sub>, 1.8 mM of CaCl<sub>2</sub> and 11.1 mM of dextrose) to remove any unbound dye. All stretching experiments were then performed in HBSS solution to maintain pH constant.

## Image Acquisition and Analysis

Phase contrast and fluorescence images were acquired on an inverted Nikon Ti-Eclipse microscope with a Plan Fluor ELWD 40 $\times$  objective and appropriate filter sets. Images were analyzed with the Ovsucle plugin [Thévenaz et al., 2011] in ImageJ to quantify the shape and orientation of cell nuclei during substrate strain. The Ovsucle plugin was employed to fit ellipses around each nucleus in the field of view and to compute nuclear orientation with respect to the horizontal axis as well as the length of the major and minor axes of the nuclear fit in all experimental conditions. The change in nuclear morphology was computed as a percentage change in length (deformation) along the major and minor axes (see Fig. S12 in Supporting Information).

## Drug Treatments

In order to study the influence of the CSK on nuclear deformation, cells were treated with either cytochalasin-D (Sigma, St. Louis, MO) or nocodazole (Sigma) to specifically depolymerize actin or tubulin, respectively. Each drug was added to the cell culture medium 15 min prior to the stretching experiment at a final concentration of 10  $\mu\text{M}$ .

## Immunofluorescence Staining

Staining for actin, microtubules, vimentin and DAPI was achieved following a previously reported protocol [Guolla et al., 2012]. In brief, for actin and microtubule staining, cells were first rinsed with warm PBS and fixed with a solution of 2% sucrose and 3.5% formaldehyde. They were per-

meabilized with warm 0.5% Triton X-100. Cells were incubated with Phalloidin Alexa Fluor 546 (Invitrogen, NY) to stain for actin. Microtubules were stained with monoclonal anti- $\alpha$ -tubulin (Sigma), then with Alexa Fluor 488 conjugated rabbit anti-mouse immunoglobins (Invitrogen, NY) for 15 min with a 15-min wash following each incubation. Lastly, nuclei were labelled by incubating with DAPI (Invitrogen, NY). For staining of vimentin, cell were also first rinsed with warm PBS but then fix and permeabilized with cold methanol (-20 °C) for 6 min. Cells were incubated with monoclonal anti-vimentin (Sigma) for 30 min, then with Alexa Fluor 488 conjugated rabbit anti-mouse immunoglobins (Invitrogen, NY) for 15 min with a 15-min wash following each incubation.

## Statistics

In total, we analyzed the nuclear deformation of 28 control cells, 31 cytochalasin-D-treated cells and 22 nocodazole-treated cells. All values are presented in average  $\pm$  SEM. One-sample *t*-test was performed to investigate the anisotropic behaviour of the nuclei. Changes in length between major and minor axis of cell were compared using a paired *t*-test. Observed major and minor axes deformations in response to compressive and non-compressive uniaxial strain fields were compared using paired *t*-tests. Observed major and minor axes deformations between untreated cells and cells treated with nocodazole and cytochalasin-D were compared using a one-way ANOVA followed by Tukey post-test. Statistical results with a *P*-value below 0.05 were considered significant.

## Acknowledgments

D.T. thanks the Fond de recherche du Québec: Nature et Technologie (FQRNT) and Mitacs Elevate Program. A.L. acknowledges support from the Natural Sciences and Engineering Research Council (NSERC) Undergraduate Student Research Award and the University of Ottawa Undergraduate Research Opportunities Program. A.E.P. acknowledges generous support from a Province of Ontario Early Research Award and a Canada Research Chair (CRC). This work was made possible by funding from an NSERC Discovery Grant, NSERC Discovery Accelerator Supplement and a CRC Operating Grant.

## References

- Anno T, Sakamoto N, Sato M. 2012. Role of nesprin-1 in nuclear deformation in endothelial cells under static and uniaxial stretching conditions. *Biochem Biophys Res Commun* 424:94–99.
- Arnoczky SP, Lavagnino M, Whallon JH, Hoonjan A. 2002. In situ cell nucleus deformation in tendons under tensile load: a morphological analysis using confocal laser microscopy. *J Orthop Res* 20: 29–35.
- Balachandran K, Alford PW, Wylie-Sears J, Goss JA, Grosberg A, Bischoff J, Aikawa E, Levine RA, Parker KK. 2011. Cyclic strain induces dual-mode endothelial-mesenchymal transformation of the cardiac valve. *Proc Natl Acad Sci USA* 108:19943–19948.

- Barker AJ, Lanning C, Shandas R. 2010. Quantification of hemodynamic wall shear stress in patients with bicuspid aortic valve using phase-contrast MRI. *Ann Biomed Eng* 38:788–800.
- Boccafoschi F, Mosca C, Bosetti M, Cannas M. 2011. The role of mechanical stretching in the activation and localization of adhesion proteins and related intracellular molecules. *J Cell Biochem* 112:1403–1409.
- Booth-Gauthier EA, Alcoser TA, Yang G, Dahl KN. 2012. Force-induced changes in subnuclear movement and rheology. *Biophys J* 103:2423–2431.
- Chiquet M, Gelman L, Lutz R, Maier S. 2009. From mechanotransduction to extracellular matrix gene expression in fibroblasts. *Biochim Biophys Acta* 1793:911–920.
- Coffinier C, Jung HJ, Nobumori C, Chang S, Tu Y, Barnes RH, Yoshinaga Y, de Jong PJ, Vergnes L, Reue K, Fong LG, Young SG. 2011. Deficiencies in lamin B1 and lamin B2 cause neurodevelopmental defects and distinct nuclear shape abnormalities in neurons. *Mol Biol Cell* 22:4683–4693.
- Crisp M, Liu Q, Roux K, Rattner JB, Shanahan C, Burke B, Stahl PD, Hodzic D. 2006. Coupling of the nucleus and cytoplasm: role of the LINC complex. *J Cell Biol* 172:41–53.
- Dahl KN, Ribeiro AJS, Lammerding J. 2008. Nuclear shape, mechanics, and mechanotransduction. *Circ Res* 102:1307–1318.
- Duprey A, Khanafer K, Schlicht M, Avril S, Williams D, Berguer R. 2010. In vitro characterisation of physiological and maximum elastic modulus of ascending thoracic aortic aneurysms using uniaxial tensile testing. *Eur J Vasc Endovasc Surg* 39:700–707.
- Frydrychowicz A, Berger A, Russe MF, Stalder AF, Harloff A, Dittrich S, Hennig J, Langer M, Markl M. 2008. Time-resolved magnetic resonance angiography and flow-sensitive 4-dimensional magnetic resonance imaging at 3 Tesla for blood flow and wall shear stress analysis. *J Thorac Cardiovasc Surg* 136:400–407.
- Goldyn AM, Rioja BA, Spatz JP, Ballestrem C, Kemkemer R. 2009. Force-induced cell polarisation is linked to RhoA-driven microtubule-independent focal-adhesion sliding. *J Cell Sci* 122:3644–3651.
- Guolla L, Bertrand M, Haase K, Pelling AE. 2012. Force transduction and strain dynamics in actin stress fibres in response to nanonewton forces. *J Cell Sci* 125:603–613.
- Haga JH, Li YSJ, Chien S. 2007. Molecular basis of the effects of mechanical stretch on vascular smooth muscle cells. *J Biomech* 40:947–960.
- Haque F, Mazzeo D, Patel JT, Smallwood DT, Ellis JA, Shanahan CM, Shackleton S. 2010. Mammalian SUN protein interaction networks at the inner nuclear membrane and their role in laminopathy disease processes. *J Biol Chem* 285:3487–3498.
- Heo SJ, Nerurkar NL, Baker BM, Shin JW, Elliott DM, Mauck RL. 2011. Fiber stretch and reorientation modulates mesenchymal stem cell morphology and fibrous gene expression on oriented nanofibrous microenvironments. *Ann Biomed Eng* 39:2780–2790.
- Herrmann H, Bär H, Kreplak L, Strelkov SV, Aebi U. 2007. Intermediate filaments: from cell architecture to nanomechanics. *Nat Rev Mol Cell Biol* 8:562–573.
- Jungbauer S, Gao H, Spatz JP, Kemkemer R. 2008. Two characteristic regimes in frequency-dependent dynamic reorientation of fibroblasts on cyclically stretched substrates. *Biophys J* 95:3470–3478.
- Khatau SB, Bloom RJ, Bajpai S, Razafsky D, Zang S, Giri A, Wu PH, Marchand J, Celedon A, Hale CM, Sun SX, Hodzic D, Wirtz D. 2012. The distinct roles of the nucleus and nucleus-cytoskeleton connections in three-dimensional cell migration. *Sci Rep* 2:488.
- Khatau SB, Hale CM, Stewart-Hutchinson PJ, Patel MS, Stewart CL, Searson PC, Hodzic D, Wirtz D. 2009. A perinuclear actin cap regulates nuclear shape. *Proc Natl Acad Sci USA* 106:19017–19022.
- Kim DH, Khatau SB, Feng Y, Walcott S, Sun SX, Longmore GD, Wirtz D. 2012. Actin cap associated focal adhesions and their distinct role in cellular mechanosensing. *Sci Rep* 2:555.
- Korfali N, Wilkie GS, Swanson SK, Srsen V, Batrakou DG, Fairley EAL, Malik P, Zuleger N, Goncharevich A, de Las Heras J, Kelly DA, Kerr ARW, Florens L, Schirmer EC. 2010. The leukocyte nuclear envelope proteome varies with cell activation and contains novel transmembrane proteins that affect genome architecture. *Mol Cell Proteomics* 9:2571–2585.
- Lammerding J, Schulze PC, Takahashi T, Kozlov S, Sullivan T, Kamm RD, Stewart CL, Lee RT. 2004. Lamin A/C deficiency causes defective nuclear mechanics and mechanotransduction. *J Clin Invest* 113:370–378.
- Maniotis AJ, Chen CS, Ingber DE. 1997. Demonstration of mechanical connections between integrins, cytoskeletal filaments, and nucleoplasm that stabilize nuclear structure. *Proc Natl Acad Sci USA* 94:849–854.
- Mazumder A, Shivashankar GV. 2010. Emergence of a prestressed eukaryotic nucleus during cellular differentiation and development. *J R Soc Interface* 7 Suppl 3:S321–330.
- Morioka M, Parameswaran H, Naruse K, Kondo M, Sokabe M, Hasegawa Y, Suki B, Ito S. 2011. Microtubule dynamics regulate cyclic stretch-induced cell alignment in human airway smooth muscle cells. *PLoS One* 6:e26384.
- Nathan AS, Baker BM, Nerurkar NL, Mauck RL. 2011. Mechano-topographic modulation of stem cell nuclear shape on nanofibrous scaffolds. *Acta Biomater* 7:57–66.
- Ngu H, Feng Y, Lu L, Oswald SJ, Longmore GD, Yin FCP. 2010. Effect of focal adhesion proteins on endothelial cell adhesion, motility and orientation response to cyclic strain. *Ann Biomed Eng* 38:208–222.
- Razafsky D, Hodzic D. 2009. Bringing KASH under the SUN: the many faces of nucleo-cytoskeletal connections. *J Cell Biol* 186:461–472.
- Reddy KL, Zullo JM, Bertolino E, Singh H. 2008. Transcriptional repression mediated by repositioning of genes to the nuclear lamina. *Nature* 452:243–247.
- Rosenzweig DH, Matmati M, Khayat G, Chaudhry S, Hinz B, Quinn TM. 2012. Culture of primary bovine chondrocytes on a continuously expanding surface inhibits dedifferentiation. *Tissue Eng Part A* 18:2466–2476.
- Shivashankar GV. 2011. Mechanosignaling to the cell nucleus and gene regulation. *Annu Rev Biophys* 40:361–378.
- Starr DA, Fridolfsson HN. 2010. Interactions between nuclei and the cytoskeleton are mediated by SUN-KASH nuclear-envelope bridges. *Annu Rev Cell Dev Biol* 26:421–444.
- Steward R, Cheng CM, Ye J, Bellin R, LeDuc P. 2011. Mechanical stretch and shear flow induced reorganization and recruitment of fibronectin in fibroblasts. *Sci Rep* 1:147.
- Sullivan T, Escalante-Alcalde D, Bhatt H, Anver M, Bhat N, Nagashima K, Stewart CL, Burke B. 1999. Loss of A-type lamin expression compromises nuclear envelope integrity leading to muscular dystrophy. *J Cell Biol* 147:913–920.
- Szcerbal I, Foster HA, Bridger JM. 2009. The spatial repositioning of adipogenesis genes is correlated with their expression status in a porcine mesenchymal stem cell adipogenesis model system. *Chromosoma* 118:647–663.
- Thévenaz P, Delgado-Gonzalo R, User M. 2011. The ovuscul. *IEEE Trans Pattern Anal Mach Intell* 33:382–393.

---

Tremblay D, Cartier R, Mongrain R, Leask RL. 2010. Regional dependency of the vascular smooth muscle cell contribution to the mechanical properties of the pig ascending aortic tissue. *J Biomech* 43:2448–2451.

Tremblay D, Zigras T, Cartier R, Leduc L, Butany J, Mongrain R, Leask RL. 2009. A comparison of mechanical properties of materials used in aortic arch reconstruction. *Ann Thorac Surg* 88:1484–1491.

Vande Geest JP, Sacks MS, Vorp DA. 2006. The effects of aneurysm on the biaxial mechanical behavior of human abdominal aorta. *J Biomech* 39:1324–1334.

Versaevel M, Grevesse T, Gabriele S. 2012. Spatial coordination between cell and nuclear shape within micropatterned endothelial cells. *Nat Commun* 3:671.

Wilhelmsen K, Litjens SHM, Kuikman I, Tshimbalanga N, Janssen H, van den Bout I, Raymond K, Sonnenberg A. 2005. Nesprin-3, a novel outer nuclear membrane protein, associates with the cytoskeletal linker protein plectin. *J Cell Biol* 171:799–810.

Yang G, Crawford RC, Wang JHC. 2004. Proliferation and collagen production of human patellar tendon fibroblasts in response to cyclic uniaxial stretching in serum-free conditions. *J Biomech* 37:1543–1550.